rotating disk case,[13] numerical results have been obtained over a range of rotation rates, scan rates, and kinetic parameters. These suggest that for S-shaped (rather than peak-shaped) voltammograms, i.e., for $p \lesssim 1.6$, and for totally irreversible reactions, the shape of the voltammogram does not change with changes in p. The maximum value of p used here was 0.45, and for most of the data, $p \leq 0.28$. Furthermore, there is no trend in the derived value of $(1 - \alpha)$ with changes in p over this range.

We conclude that for voltammograms with only modest contribution of transient current ($\lesssim 5\%$) the systematic error introduced by treating the voltammograms as steady-state ones is not larger than the usual experimental errors.

Finally, we examine the reasonableness of the assumption that the current density is uniform. In 0.1 M H_2SO_4, the specific conductance, κ, is ca. 0.04 ohm^{-1} cm^{-1} and the currents are in the low nanoampere range. Thus, concentration and charge-transfer polarization should predominate over Ohmic polarization, and the distribution of current should be uniform. Quantitatively, deviations from uniformity should be negligible for $J, \Delta \ll 1$, where J and Δ are normalized exchange current density and average current density, respectively:[14] $J = i^\circ z f r_0/\kappa$; $\Delta = |i_{av}| z f r_0/\kappa$. For the present case $z = 2$ and $J \leq 0.003$, $\Delta \leq 0.002$. We conclude that the assumption of uniform current density is reasonable.

The procedure is summarized as follows. Conditions of step height and step width (or scan rate) and electrode radius are sought for which S-shaped voltammograms are obtained, as illustrated in Figure 1. Data are obtained for a range of radii and step width (scan rate) to verify that the limiting current behaves according to theory and that the operating conditions are acceptably close to the steady state, as illustrated in Table I. Voltammograms are then analyzed according to eq 12 (Figure 3) or eq 14 (Figures 4 and 5), making use of an independently measured value of $E^r_{1/2}$ and the value of D obtained from the limiting steady-state current.

Acknowledgment. We thank John O'Dea for assisting with the instrumentation. This work was supported in part by the Office of Naval Research.

Registry No. Fe, 7439-89-6; Pt, 7440-06-4; H_2SO_4, 7664-93-9.

(13) Lovric, M.; Osteryoung, J. G. *J. Electroanal. Chem.* **1986**, *197*, 63-75.

(14) Newman, J. *J. Electrochem. Soc.* **1966**, *113*, 1235-1241.

Dipole–Dipole Induced Forces in the Reaction of Alkali Metal Atoms with Polar Molecules

Yu-Ran Luo and Sidney W. Benson*

Donald P. and Katherine B. Loker Hydrocarbon Research Institute, University of Southern California, University Park mc-1661, Los Angeles, California 90089 *(Received: September 19, 1986; In Final Form: August 27, 1987)*

The title reaction is shown to be dominated by a relatively large dipole–dipole induced interaction at distances of 4–5 Å. The cone of nonreaction and orientation dependence of the reactive scattering cross section are estimated from this potential. The dipole–dipole induced potential is shown to strongly favor the observed head-on reaction.

Introduction

About 20 years ago Bernstein[1] and Brooks[2] first reported the preliminary results from a crossed-beam study of the reactions of Rb and K with partially oriented CH_3I. This stimulated much interest in the study of the microscopic aspects of oriented molecule reactions using both hexapole electrostatic fields[3-6] and photoselection techniques.[7-9] At the same time there have been several theoretical analyses[10-20] of the orientation dependence.

The present paper uses a dipole–dipole induced potential to analyze the steric effects of the oriented reactions of alkali metal atoms (K, Rb) with polar molecules and to propose a spherical particle model which gives theoretical results in agreement with these observations.

Model

The reactions of alkali metal atoms with methyl iodide have been studied at thermal energies by a wide variety of experimental techniques.[21,22] It is known that for these reactions there is a very low ($\lesssim 8$ kJ mol^{-1}) or zero barrier on the potential energy surface. The product MI is backscattered relative to the incident M atom in the center-of-mass system of M + CH_3I (the so-called "rebound mechanism").[23] For Rb + CH_3I, it has been found[24]

(1) Beuhler, Jr., R. J.; Bernstein, R. B.; Kramer, K. H. *J. Am. Chem. Soc.* **1966**, *88*, 5331.
(2) (a) Brooks, P. R.; Jones, E. M. *J. Chem. Phys.* **1966**, *45*, 3448. (b) Marcellin, G.; Brooks, P. R. *J. Am. Chem. Soc.* **1975**, *97*, 1710.
(3) Brooks, P. R. *Science* **1976**, *193*, 11 and cited references.
(4) Parker, D. H.; Chakravorty, K. K.; Bernstein, R. B. *J. Phys. Chem.* **1981**, *85*, 466; *Chem. Phys. Lett.* **1982**, *86*, 113.
(5) Stolte, S.; Chakravorty, K. K.; Bernstein, R. B.; Parker, D. H. *Chem. Phys.* **1982**, *71*, 353.
(6) Stolte, S. *Ber. Bunsen-Ges. Phys. Chem.* **1982**, *86*, 413 and cited references.
(7) Estler, R. C.; Zare, R. N. *J. Am. Chem. Soc.* **1978**, *100*, 1323.
(8) Karny, Z.; Zare, R. N. *J. Chem. Phys.* **1978**, *68*, 3360.
(9) Karny, Z.; Estler, R. C.; Zare, R. N. *J. Chem. Phys.* **1978**, *69*, 5199.
(10) Karplus, M.; Godfrey, M. *J. Am. Chem. Soc.* **1966**, *88*, 5332.
(11) Levine, R. D.; Bernstein, R. B. *Molecular Reaction Dynamics*; Clarendon: Oxford, 1974.
(12) Smith, I. W. M. *J. Chem. Educ.* **1982**, *59*, 9.
(13) Blais, N. C.; Truhlar, D. G. *Chem. Phys. Lett.* **1983**, *102*, 120.
(14) Engel, Y. M.; Levine, R. D. *Chem. Phys.* **1984**, *91*, 167.
(15) Levine, R. D.; Bernstein, R. B. *Chem. Phys. Lett.* **1984**, *105*, 467.
(16) Blais, N. C.; Bernstein, R. B.; Levine, R. D. *J. Phys. Chem.* **1985**, *89*, 10.
(17) Evans, G. T.; She, P. S. C.; Bernstein, R. B. *J. Chem. Phys.* **1985**, *82*, 2258.
(18) Bernstein, R. B. *J. Chem. Phys.* **1985**, *82*, 3656.
(19) Choi, S. E.; Bernstein, R. B. *J. Chem. Phys.* **1985**, *83*, 4463.
(20) Blais, N. C.; Bernstein, R. B. *J. Chem. Phys.* **1986**, *85*, 7030.
(21) Davidovits, P.; McFadden, D. L. *Alkali Halide Vapors*; Academic: New York, 1979.
(22) Levy, M. R. *Prog. React. Kinet.* **1979**, *10*, 1.

0022-3654/88/2092-1107$01.50/0

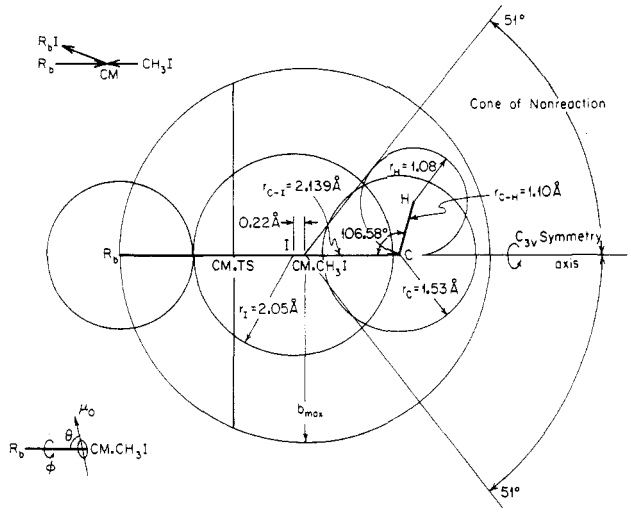

Figure 1. Scaled representation of the steric effect of the Rb + CH_3I reaction. The van der Waals radii are taken from ref 25 and 26, respectively, and the structural data for CH_3I from ref 27. CM is the center of mass, CM.TS is the center of mass of the transition state, and CM.CH_3I is the center of mass of CH_3I. The bond length of Rb–I in gas is 3.18 Å, and $r_{vdw}(Rb) + r_{vdw}(I) \simeq 4.5$ Å.

that the reaction cross section appears to show a narrow maximum at about 0.1-eV relative translational energy. From 0.3 to about 1.7 eV the cross section is nearly constant and half its maximum value.

The reaction dynamics of Rb + CH_3I have been found to be quite different for two possible orientations. For the CH_3 and toward Rb ("tails configuration"), there is a steric cone of nonreaction, whereas for the I end toward Rb ("heads configuration"), the orientation is favorable and the product RbI is backscattered. This indicates that the steric effect is due to the nonreactive CH_3 end of the methyl iodide molecule. Perhaps the most surprising feature of the angular dependence is that it is a maximum on the symmetry axis and a minimum at 120° as we approach the CH_3 group. Purely geometrical factors would have suggested the opposite trend.

Bernstein and colleagues have used orientational opacity functions to determine the cutoff angle of this nonreactive cone. For a new improved opacity function[19] the cutoff half-angle of the steric cone which is blocked out by the methyl group in the course of a reactive collision was found to be 53 ± 2° at 13 kJ mol^{-1}.

Figure 1 represents a "head-on" collision and illustrates the steric effect on the Rb + CH_3I reaction. There is a steric cone of nonreaction due to the unreactive methyl end of the CH_3I molecule. If a tangent is drawn from the center of mass of the methyl iodide molecule to the spheres with radii equal to that of the van der Waals radii of the three hydrogen atoms, then it is possible to estimate the cone angle, which is about 51°. This estimated angle is in good agreement with the most exact observation of 53 ± 2°.

If the tangent is drawn from I atom, then the estimated cutoff angle is about 47° for Rb + CH_3I. Blais and Bernstein[20] assumed the angle for K + CH_3I is 48°, the same as that for Rb + CH_3I, using a purely empirical potential energy surface. Because the van der Waals radii are available,[25-27] the tangent method for determining the cutoff angle is very simple and intuitive and in fact was employed in the earliest descriptions of the reaction.

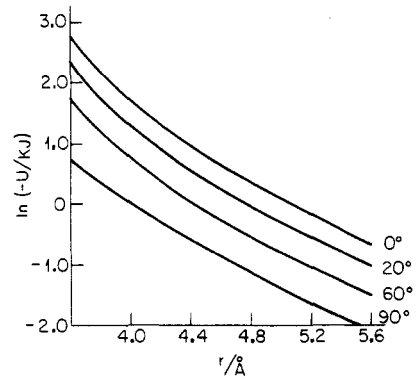

Figure 2. Dipole–dipole induced potential for the Rb–CH_3I system.

The Potential of Interaction

The interaction between the alkali metal atoms and CH_3I has been described as a classical, hard-sphere encounter[28,29] and also by the harpoon or electron jump model.[30] The long-range molecular interactions may be divided into three types: direct dipole–dipole, dipole–induced dipole, and induced dipole–induced dipole (dispersion force). For the title reactions, the dipole–dipole force is zero.[31] Rothe and Bernstein's calculations suggest that the dispersion force is an order of magnitude larger than the dipole–induced dipole contribution for the reaction Rb + CH_3I. However, the Slater–Kirkwood equation for the dispersion force is not useful for alkali metal atom systems. The dispersion contribution is estimated at over 110 kcal mol^{-1} at van der Waals contact between two Rb atoms according to the Slater–Kirkwood equation. This is about 10 times the Rb–Rb bond energy.

CH_3I has an important dipole moment, $\mu_0 = 1.62$ D, while more significant is the fact that alkali metal and alkaline earth metal atoms have surprisingly large polarizabilities in the range 20–50 $Å^3$. This is far in excess of what might be anticipated from their ionization potentials or from the classical formula for a conducting sphere. One consequence of this large polarizability is that we will have significant dipole–dipole induced forces acting out to distances of 5 Å.

If we consider for example a much simplified model with a point dipole centered at the I atom nucleus, then the Rb atom, approaching along the C–I symmetry axis, will experience a purely radial force along this axis. The dipole induced in the Rb atom is

$$\mu_{Rb} = \frac{2\mu_0\alpha_M/r^3}{1 - 4\alpha_M\alpha_I/r^6} \quad (1)$$

where α_M and α_I are the atom polarizabilities of M and I, respectively. The denominator in eq 1 arises from the back-polarization of the I atom by μ_M and becomes significant even at 5 Å.

At any arbitrary angle of approach θ of the Rb atom to the direction of the dipole μ_0 (see Figure 1), there will be an electric field $\vec{E}$ acting on Rb with components along the polar directions r and θ given by

$$E_r = \frac{2\mu_0 \cos\theta/r^3}{1 - 4\alpha_I\alpha_M/r^6} \qquad \vec{E}_\theta = \frac{\mu_0 \sin\theta/r^3}{1 - \alpha_I\alpha_M/r^6} \quad (2)$$

This electric field is quite strong. For Rb + CH_3I, $\theta = 0°$, $r = 6$ Å, and $\vec{E}_r = 4.6 \times 10^7$ V cm^{-1}, while at $r = 10$ Å, $\vec{E}_r = 9.8 \times 10^6$ V cm^{-1}; if one uses $\mu_0 = 1.62$ D for CH_3I,[26] $\alpha_{Rb} = 47.3 \times 10^{-30}$ m^3 [29] and $\alpha_I = 3.9 \times 10^{-30}$ m^3.[32] The dipole moments

(23) Bernstein, R. B. *Chemical Dynamics via Molecular Beam and Laser Techniques*; Clarendon: Oxford, 1982.
(24) Wu, K. T.; Pang, H. F.; Berstein, R. B. *J. Chem. Phys.* **1978**, *68*, 1064.
(25) Weast, R. C., Ed. *CRC Handbook of Chemistry, and Physics*, 57th ed.; CRC: Boca Raton, FL, 1976.
(26) Motoc, I.; Marshall, G. R. *Chem. Phys. Lett.* **1985** *116*, 416 and cited references.
(27) *Tables of Interatomic Distances and Configurations in Molecules and Ions*, Special Publications No. 18; The Chemical Society: London, 1965.
(28) Shin, H. K. *Chem. Phys. Lett.* **1977**, *43*, 533; **1975**, *38*, 253; **1975**, *34*, 596.
(29) Urena, A. G.; Aoiz, F. *J. Chem. Phys. Lett.* **1977**, *51*, 281.
(30) Wu, K. T. *J. Phys. Chem.* **1979**, *83*, 1043.
(31) Rothe, E. W.; Bernstein, R. B. *J. Chem. Phys.* **1959**, *31*, 1619.

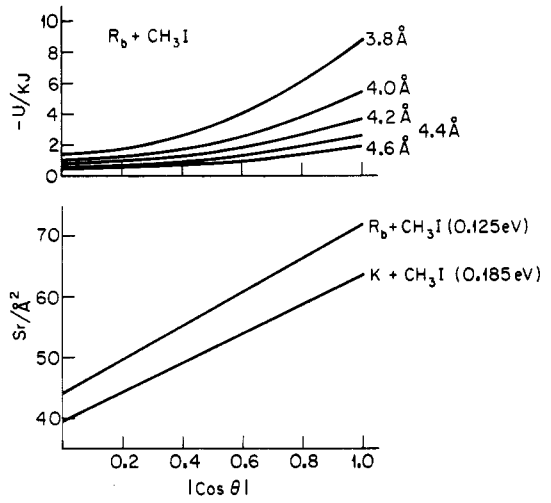

Figure 3. (a, top) Angular dependence of the potential. (b, bottom) Estimated cross sections as a function of angle for Rb + CH_3I at 0.125 eV and for K + CH_3I at 0.185 eV.

induced in the Rb atom are 0.72 and 0.15 D for the two cases, respectively.

The total interaction energy is given by

$$U(r,\theta) = -\frac{\mu_0\alpha_M}{2r^6}\left[\frac{4\cos^2\theta}{(1-4\alpha_I\alpha_M/r^6)^2} + \frac{\sin^2\theta}{(1-\alpha_I\alpha_M/r^6)^2}\right], \quad 0 \le \theta \le 129° \quad (3)$$

small for $r \ge r_{vdw}$, large and attractive for $r < r_{vdw}$

where 129° is the difference between 180° and the cutoff angle. We see that $U(r,\theta)$ has a strong angular dependence falling by at least a factor of 4 from $\theta = 0$ to $\theta = 90°$. This interaction produces a torque on the CH_3I dipole as well as on the Rb–ICH_3 system, tending to orient[36] them toward the $\theta = 0$ (head-on) approach. Figure 2 shows how the potential $U(r,\theta)$ falls with increasing r at a few selected angles.

Figure 3a shows the angular dependence of the potential. The curvature become monotonically smaller as r increases. This implies that the dipole–dipole induced potential at the given ranges develops slowly. The van der Waals contact $r_{vdw} \simeq 4.5$ Å.

The angular dependence of $U(r,\theta)$ makes it impossible to attempt a rigorous, closed-form solution to the collision dynamics. However, we can attempt an approximate solution by some simplifications.

Collision Dynamics

The moment of inertia of CH_3I about the symmetry axis is so small ($\sim 1/20$) relative to the two major moments that it may be looked upon as nearly a diatomic molecule with its dipole moment approximately at right angles to its angular momentum vector. As metal atom, M, approaches the I atom, the rotational angular momentum vector will begin to process about the M–I axis and the resultant torques will tend to align the M–I and C–I axes. Also, because the relative collision energies studied were in the range 0.15–1.5 eV while the ambiently determined MeI rotational energy was about $RT = 0.026$ eV, the dynamics tend to be dominated by the collision energy. Note also that the impact parameters are in the range of at least 3.5 Å while the C–I distance is only 2.14 Å so that the collision angular momentum was usually larger than the rotational angular momentum.

We now use the conservation of energy equation

$$E_c^\circ = \frac{1}{2}\mu_c\dot{r}^2 + E_c^\circ\left(\frac{b^2}{r^2}\right) + U(r,\theta) \quad (4)$$

where E_c° is the initial, center-of-mass collision energy, b the impact parameter, r the M–(CH_3I) center-of-mass separation, and μ_c the reduced mass of the collision pair. The conditions that there now occur a hard-sphere M–I collision require that, at some maximum value of $b = b_{max}$, $\dot{r} \le 0$ at the distance of closest approach r_c where the relative radial force $\bar{F}_r$ on the collision pair is less than or equal to zero. Hence, taking the derivative of both sides of eq 4 with respect to r to obtain $\bar{F}_r = 0$, we can get the critical distance $r_c(E_c^\circ,\theta)$, $b_{max}(E_c^\circ,\theta)$, and the reaction cross section $S_r(E_c^\circ,\theta)$. The data in Table I are one of the examples at low collision energy for the reaction Rb + CH_3I. These are calculated on the assumption that there is no intrinsic barrier to the reaction. The ad hoc potential used by Bernstein et al.[19,20] assumes an intrinsic barrier increasing with θ. There is no experimental evidence for such a barrier.

TABLE I: Angular Dependence of the Cross Section as a Function of Angle for Rb + CH_3I at 0.125-eV Energy

	0°	20°	40°	60°	75°	90°	129°
$r_c(\theta)$/Å	4.15	4.11	3.98	3.77	3.54	3.29	3.88
$U(r_c,\theta)$/kcal	0.96	0.94	0.90	0.83	0.83	0.96	0.85
$b_{max}(\theta)$/Å	4.79	4.73	4.56	4.23	4.02	3.80	4.42
$S_r(\theta)$/Å^2	72.0	70.3	65.2	57.3	50.8	45.4	61.3

It has been found that there is approximately a linear dependence of $S_r(\theta)$ on cos θ for the title reactions, as shown in Figure 3b. Recently, Blais and Bernstein[20] have found a similar orientational dependence of the reaction cross section for K + CH_3I, taking a purely empirical and quite detailed potential energy surface. To account for the angular dependence of the cross section, they have had to introduce an ad hoc assumption that the activation barrier increases linearly with cos θ; $A + B(1 - \cos\theta)$.

At high collision energy b_{max} should be the sum of van der Waals radii of the alkali metal atom and the iodine atom. For reactions of Rb and K, they are 4.50 and 4.35 Å, respectively. But the observed cross section should be an average one. That is

$$S_{r,obsd}\ (\text{high energy}) \simeq \frac{1}{4\pi}\int \pi r_{vdw}^2\, d\phi$$

$$= \frac{\pi}{2} r_{vdw}^2 \simeq 30\ Å^2$$

This estimated value is about half of the reactive cross section at low collision energy (see Table I).

Discussion

While one might expect a similar behavior for CF_3I and CF_3Br, the smaller dipole moments in these molecules make the induced forces negligibly small at the values of E_c° used since they depend on μ^2. For these the harpoon mechanism gives larger cross sections[33-35] than that expected for CH_3I since the electron affinities of CF_3Br and CF_3I are both about 1.57 and 0.91 eV, respectively, while that of CH_3I is negligibly small at 0.2 ± 0.1 eV.

The polarization forces discussed here have been treated in a very approximate form. A more rigorous treatment would have to take into account the London's dispersion force which in some range may be comparable to the polarization forces. However, they would not be expected to show angular dependence except for an assymetry between the CH_3 and the I atom, being stronger for I. Their distance dependence would go as r^{-6} so that including

(32) Miller, T. M.; Bederson, B. *Adv. At. Mol. Phys.* **1977**, *13*, 1.

(33) Brooks, P. R.; Mikillop, J. S.; Pipin, H. G. *Chem. Phys. Lett.* **1979**, *66*, 144.

(34) Pauluth, M.; Rotzoll, G. *Chem. Phys. Lett.* **1984**, *111*, 238.

(35) Carman, H. S.; Harland, P. W.; Brooks, P. R. *J. Phys. Chem.* **1986**, *90*, 944.

(36) In the absence of a collision, there is no relaxation process which would produce reorientation of the colliding pair. However, the stray electric fields would cause significant precision of the CH_3I top about the I–metal axis. The laboratory fields are insigificant compared to the particle fields at $r \le 100$ Å. Note that the forces acting on the metal and I atoms will cause radial approach of these two, producing some effective reorientation.

them would produce a small enhancement at low energy in the total cross section.

Acknowledgment. We are grateful to Drs. C. D. Eley and S. S. Parmar for their helpful discussions. This work was supported by grants from the U.S. Army Research Office and the National Science Foundation.

Registry No. Rb, 7440-17-7; CH_3I, 74-88-4; BH_3, 13283-31-3; CO, 630-08-0; NO, 10102-43-9; C_2H_4, 74-85-1; O_2, 7782-44-7; H_2O, 7732-18-5.

Scaling Relations and Self-Similarity Conditions in Strongly Coupled Dynamical Systems

Herschel Rabitz*

Department of Chemistry, Princeton University, Princeton, New Jersey 08544

and Mitchell D. Smooke

Department of Mechanical Engineering, Yale University, New Haven, Connecticut 06520
(Received: September 23, 1986)

Dynamical equations arising in a number of physical areas typically involve many dependent variables as well as numerous parameters. In some cases these equations may contain a dominant dependent variable (e.g., the temperature in flame systems, etc.), and the consequences of such an identification are examined in this paper. Particular emphasis is placed on the behavior of dynamical Green's functions and system sensitivity coefficients with respect to the parameters residing in the particular model. In the case of a single dominant dependent variable for a system of ordinary differential equations, it is possible to reduce the Green's function matrix to knowledge of one of its columns and often to one independent element. Furthermore, when there are N dependent variables and M parameters, the $N \times M$ matrix of sensitivity coefficients reduces to knowledge of only two characteristic vectors of lengths N and M, respectively. These various reductions are referred to as scaling relations and self-similarity conditions. The consequences of a dominant dependent variable are illustrated with examples drawn from various areas of combustion and kinetics modeling. A brief discussion in the Appendix is also presented on similar organizing principles in multidominant dependent variable systems and cases described by partial differential equations.

I. Introduction

Mathematical modeling in a host of physical areas is becoming an increasingly powerful tool for analysis and design purposes. A natural consequence of these developments has been the increased interest in employing sensitivity analysis tools for probing the role of physical parameters residing in a particular model under study.[1] A growing literature exists in the latter area with extensive numerical calculations becoming available. In many respects the numerical sensitivity analysis calculations are providing a data base from which to seek out any generic or general trends transcending particular physical systems or problems. The existence of such rules of thumb could be extremely important for providing a basis for simplifying complex systems and perhaps even interrelating different models of the same process. We will refer in this paper to connections of this type as scaling and self-similarity relations among the system's dependent and independent variables. By definition, the dependent variables are those whose solution is sought in the modeling process and the independent variables are those parameters residing in the equations, boundary conditions, or initial conditions. For purposes of physical clarity the independent coordinates or time will be distinguished from the parameters themselves.

The basic thesis of this paper is that scaling relations and self-similarity conditions may occur in dynamical systems where one or, at most, a few dependent variables dominate the physical behavior of the remainder. Situations like this may arise in a number of circumstances with the case of combustion receiving particular attention in this paper. In combustion problems the temperature is a natural controlling variable if it varies appreciably over the spatial and/or temporal range of interest. The dominant role of the temperature has been long recognized in combustion. Although combustion phenomena motivated the developments described below, the conclusions may also apply to other problems where similar controlling dependencies occur. We will show that a dominant dependence has fundamental consequences for the relationship between all the dependent variables and parameters of a system.

To provide some necessary background on the development of the dominant variable scaling and self-similarity conditions, a brief introduction to the relevant aspects of sensitivity analysis will be presented in section II. This will be followed by the derivation of the scaling relations and self-similarity conditions in section III for problems described in terms of ordinary differential equations with a single dominant dependent variable. The approach taken is based on the presentation of a critical conjecture upon the form of the kinetic solutions (cf. eq 10a), and the sensitivity consequences are then developed. The justification of the conjecture resides in its successful prediction of sensitivity behavior under appropriate conditions. An accompanying Appendix will give an introduction to an extension of the theory into the realm of multidominant dependent variables and cases described by partial differential equations. Some illustrations will be given in section IV and more extensive examples will be presented elsewhere covering the detailed physical aspects of the problems. Finally, in section V we present some concluding comments.

II. Basic Operating Equations

Sensitivity analysis concepts are central to the issues of this paper. As a result, a summary of germane aspects of the theory will be presented here for completeness. A specific physical problem of interest concerns the study of steady premixed laminar flames.[2] Realistic laboratory situations of this type may be

(1) (a) Tomovic, R.; Vukobratovic, M. *General Sensitivity Theory*; American Elsevier: New York, 1972. (b) Tilden, J.; Costanza, V.; McCrae, J.; Seinfeld, J. In *Modelling of Chemical Reaction Systems*; Ebert, K., Deuflhard, P., Jager, W., Eds.; Springer-Verlag: Berlin, 1981. (c) Rabitz, H.; Kramer, M.; Dacol, D. *Annu. Rev. Phys. Chem.* **1983**, *34*, 419. Rabitz, H. *Chem. Rev.* **1987**, *87*, 101.

(2) Buckmaster, J. D.; Ludford, G. S. S. *Theory of Laminar Flames*; Cambridge University Press: London, 1982.

0022-3654/88/2092-1110$01.50/0